Draft version December 7, 2015
Preprint typeset using LaTeX style emulateapj v. 01/23/15

CLUSTER DYNAMICS WITH HETDEX - I: SIMULATED PERFORMANCE, MASS DISTRIBUTION AND LIMITS

Steven Boada[1], C. Papovich[1], and R. Wechsler[2,3]

Draft version December 7, 2015

ABSTRACT

ABSTRACT GOES HERE!! Lorem ipsum dolor sit amet, consectetur adipisicing elit, sed do eiusmod tempor incididunt ut labore et dolore magna aliqua. Ut enim ad minim veniam, quis nostrud exercitation ullamco laboris nisi ut aliquip ex ea commodo consequat. Duis aute irure dolor in reprehenderit in voluptate velit esse cillum dolore eu fugiat nulla pariatur. Excepteur sint occaecat cupidatat non proident, sunt in culpa qui officia deserunt mollit anim id est laborum.

Subject headings:

1. INTRODUCTION

Our ability to perform precision cosmology with clusters of galaxies has reached a critical turning point. The widely accepted ΛCDM model of cosmology makes explicit predictions about the number and masses of galaxy clusters throughout the universe. However, connecting these predictions to a set of, sufficiently large in size, observed clusters remains a principal problem. Specifically, the largest threat to modern, precision, cluster cosmology is not the identification of large numbers of clusters (the total number of clusters known is only going up) but the accurate recovery of galaxy cluster mass (e.g., Sehgal et al. 2011; Planck Collaboration 2013; Bocquet et al. 2015).

As mass is not a direct observable, a lot of work is underway to characterize galaxy cluster masses with an observable feature of galaxy clusters. The goal is to constrain, as best possible, $P(X|M,z)$ the probability (P) that a galaxy cluster of given mass (M), located at redshift (z) determined using observable parameter (X). The observable parameter most commonly observed X-ray temperatures and luminosities (e.g., Mantz et al. 2010; Rykoff et al. 2014; Mantz et al. 2015), cosmic microwave background observations (e.g., Vanderlinde et al. 2010; Sehgal et al. 2011) using the Sunyaev–Zeldovich effect (SZE; Sunyaev & Zeldovich 1972) or optical studies (e.g., Rozo et al. 2010, 2015) of richness (e.g., Abell 1958; Rykoff et al. 2012) or galaxy velocity dispersions (e.g., Ruel et al. 2014; Sifón et al. 2015).

Massive surveys, both on going and planned, are revolutionizing cluster cosmology using a large range of wavelengths. The South Pole Telescope (SPT; Carlstrom et al. 2011) and the Atacama Cosmology Telescope (ACT; Swetz et al. 2011) are discovering many clusters through the SZE. Optically, the on going The Dark Energy Survey (DES; The Dark Energy Survey Collaboration 2005) and planned Large Synoptic Survey Telescope (LSST; LSST Dark Energy Science Collaboration 2012) will identify many thousands of clusters to much lower masses than is possible with SZE measurements. However, regardless of the discovery method used, spectroscopic followup is needed to further constrain $P(X|M,z)$. But as the cluster dataset grows to many tens of thousands of clusters individual followup becomes increasingly impractical. Therefore, large spectroscopic surveys are needed to more fully constrain the observable–mass relation of clusters.

The Hobby Eberly Telescope Dark Energy eXperiment (HETDEX; Hill et al. 2008) is a trailblazing effort to observe high-redshift large scale structures using cutting edge wide-field integral field unit (IFU) spectrographs. Designed to probe the evolution of the dark energy equation of state etched onto high redshift ($z > 2$) galaxies by the Baryon Acoustic Oscillations (Eisenstein et al. 2005) in the first moments of the universe, the survey will observe two fields for a total of 420 degree^2 from two fields (300 degree^2, Spring field and 120 degree^2, Fall field). Tuned to find Lyα emitting (LAE) galaxies at $1.9 < z < 3.5$, HETDEX expects to find 800,000 LAEs, and more than one million [O II] emitting galaxies at $z < 0.5$ masquerading as high-redshift galaxies (Acquaviva et al. 2014).

While a large portion of the $\sim 10^6$ interloping [O II] galaxies will be field (not associated with a bound structure) galaxies, the large area covered by HETDEX is expected to contain as many as 100 Virgo-sized ($M_{dyn} \sim 10^{15}$ $M_\odot$) clusters at $z < 0.5$ (citation?). The near-complete spectroscopic coverage allows an unprecedentedly detailed look at a very large number of clusters ranging from group scales to the very massive. In addition to the recovery of accurate dynamical masses, detailed investigations of the of dynamical state of the clusters is possible.

Connecting the dynamical properties derived from spectroscopy to the properties inferred from other studies insures the greatest impact on future work. HETDEX overlaps with the Sloan Digital Sky Survey (SDSS; Blanton et al. 2001), SDSS stripe 82 (Annis et al. 2014), the Dark Energy Survey (DES; The Dark Energy Survey Collaboration 2005), and the upcoming DECam/IRAC Galaxy Environment Survey (DIRGES; PI: Papovich, C. Papovich et al. in preparation). SHELA and others?

[1] George P. and Cynthia Woods Mitchell Institute for Fundamental Physics and Astronomy, and Department of Physics and Astronomy, Texas A&M University, College Station, TX, 77843-4242; boada@physics.tamu.edu
[2] Kavli Institute for Particle Astrophysics and Cosmology, Department of Physics, Stanford University, Stanford, CA 94305, USA
[3] Department of Particle Physics and Astrophysics, SLAC National Accelerator Laboratory, Menlo Park, CA 94025, USA

Would be good to have a whole list of different things and different wavelengths. While the potential dataset is very rich, two large issues remain.

It is unclear how a blind spectroscopic survey with an IFU will effect the recovery of galaxy cluster dynamical properties. Unlike many previous large cluster surveys (e.g., Milvang-Jensen et al. 2008; Robotham et al. 2011; Sifón et al. 2015) which use multi-object spectrographs, the Visible Integral-Field Replicable Unit Spectrograph (VIRUS; Hill et al. 2012) used by HETDEX samples the sky unevenly which could excluded member galaxies which would otherwise be included. Secondly, it is not straightforward to use spectroscopic redshifts predominately from emission-line galaxies to interpret the kinematic and dynamical states of the clusters.

This work plans to address these concerns in the following ways. We use simulated observations which target individual galaxy clusters to investigate the recovery of parameters with such observations. Secondly, we create and evaluate a HETDEX like selection "function" of galaxies over a similarly large portion of the sky and use well adopted techniques to recover the dynamical properties, such as velocity dispersion and mass. Each observation strategy will further be constrained with "ideal" and "realistic" knowledge. Ideal knowledge assumes that we know which individual galaxy is assigned to which cluster. With realistic knowledge this is unknown and must be determined prior to the estimation of the cluster properties. Both of these strategies will better allow future work to predict the number and types of galaxy clusters which should be observed with VIRUS during both the HETDEX survey portion and through targeted follow up observations.

Give outline of paper section.

Throughout this paper, we adopt the following cosmological model ($\Omega_\Lambda = 0.77$, $\Omega_M = 0.23$, $\sigma_8 = 0.83$ and $H_0 = 72$ km s^{-1}Mpc^{-1}), assume a Chabrier initial mass function (IMF; Chabrier 2003), and use AB magnitudes (Oke 1974).

2. DATA AND MOCK OBSERVATIONS

Blah blah intro stuff...

2.1. *The "Buzzard" Catalogs*

The "Buzzard" mock galaxy catalogs (R. Wechsler et al., private communication) cover 375.68 degree^2 between $60 < RA < 90$ and $-61 < DEC < -41$ and are derived from a combination of Sub-halo Abundance Matching (ShAM) and ADDSEDs (Adding Density Dependent Spectral Energy Distributions) tied to an in house n-body cosmological simulation. A brief description of the catalog creation is described as follows. The initial conditions are generated with a second-order Lagrangian perturbation theory using `2LPTic` (Crocce et al. 2006). Dark matter (DM) n-body simulations are run using `LGadget-2` (a version of `Gadget-2`; Springel 2005). The DM halos are identified using the `ROCKSTAR` halo finder (Behroozi et al. 2013) which also calculates halo masses and other various parameters.

Galaxy M_r luminosities are added to the velocity peaks using ShAM (Reddick et al. 2013), and ADDSEDs (Adding Density Dependent Spectral Energy Distributions) assign luminosities in the other bands. A M_r-density-SED relation is created using a SDSS training set, and for each mock galaxy the SED of a randomly selected training set galaxy which has a similar M_r and density is assigned. The result is a 398.49 sq. degree mock catalog occupying a $60 \leq RA \leq 90$ and $-40 \leq DEC \leq -61$ portion of the sky. It contains 238 million galaxies with r mag < 29 and $z \leq 8.7$.

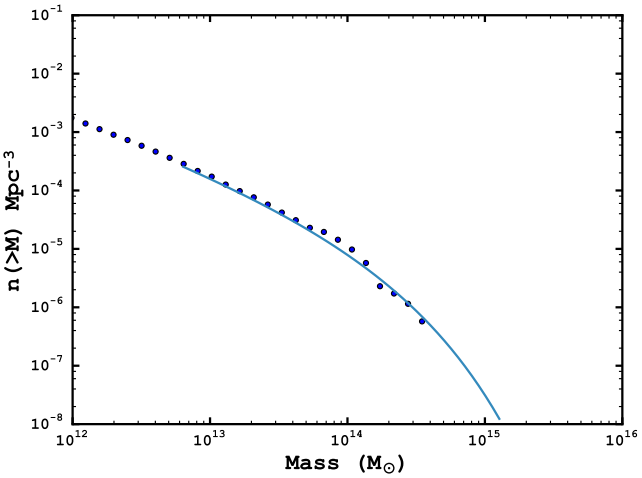

FIG. 1.— The cumulative MF of halos above M_{200c} at $z = 0.1$. The predicted MF is from Tinker et al. (2008).

The catalog information, used in this study, is broken into two large portions. The "truth" files contain the characteristics of each individual galaxies, such as right ascension (RA), declination (DEC), redshift (z), observed and rest-frame magnitudes, and many others. The "halo" files contain information for individual halos, to which many individual galaxies may belong. This includes five estimations of dynamical mass, RA, DEC, z, three dimensional velocity dispersion, and many others.

However, the catalogs do not include information on emission or absorption lines or estimations of whether the halo is relaxed or not. We supplement the catalogs with this information and describe the method in Section 2.2 and others.

We investigate the accuracy of the halo mass distribution by comparing the cumulative number density of halos above a mass (M_{200c}) threshold to the halo mass function (HMF) of Tinker et al. (2008). Shown in Figure 1 the HMF is calculated at central redshifts of 0, 0.2, and 0.4 using `HMFcalc` (Murray et al. 2013) and compared to galaxies in a redshift window of $\Delta z \pm 0.01$. We find a very good agreement between the expected HMF and the observed.

2.2. [O II] *Luminosity*

The Buzzard "truth" catalog does not provide [O II] luminosities so we must assign them empirically. We use 503113 galaxies from the SDSS Data Release 12 (Alam et al. 2015) from $z = 0.05 - 0.2$, which are selected with no redshift warning, and place each galaxy on a color-magnitude diagram (CMD) of M_r and $g-r$, see Figure 2.

To assign an [O II] luminosity to each galaxy in our catalog we place the catalog galaxies on the same CMD and select all SDSS galaxies in a small 2D (M_r, $g-r$) bin around the galaxy. We extract all of the SDSS galaxies inside that bin and create a histogram of their [O II] luminosities. Using a slice sampling technique (Neal 1997)

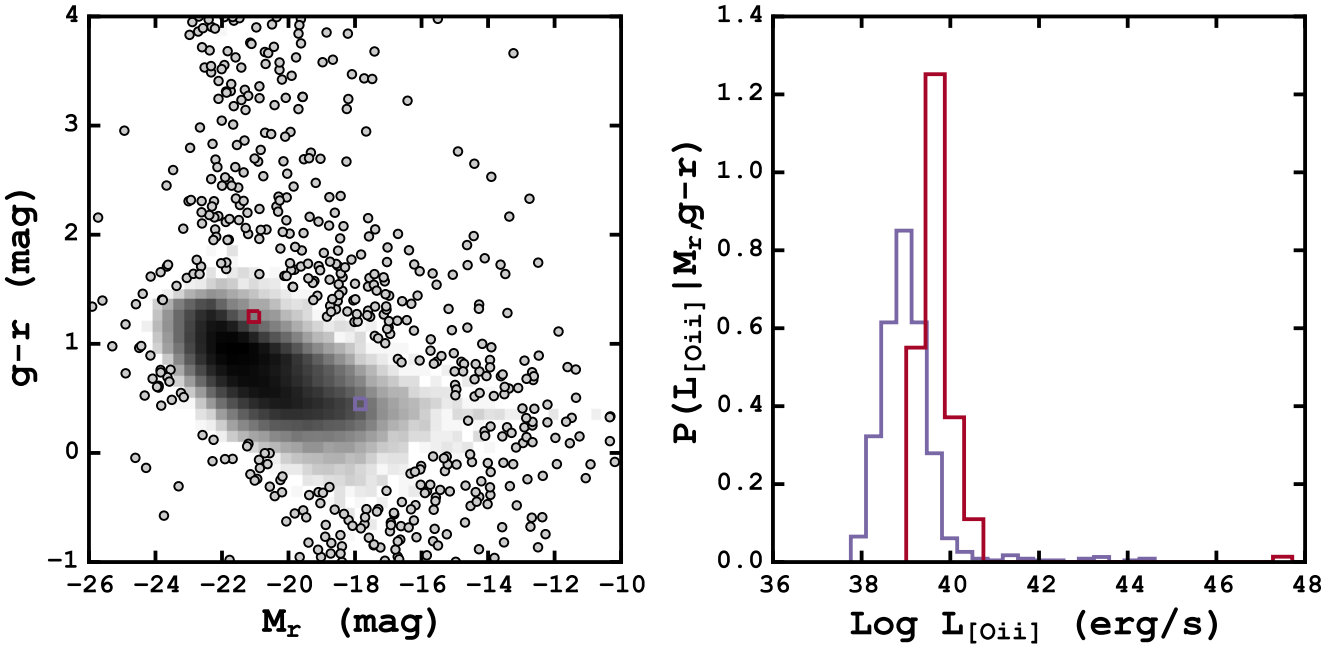

FIG. 2.— *Left*: CMD of 503113 $z < 0.2$ galaxies take from the SDSS DR12 where the shading scales with the density of points. The two boxes show regions containing potential catalog galaxies. *Right*: Probability histograms of the Log [O II] luminosity for the SDSS galaxies located in the two highlighted regions on the right. New [O II] luminosity (and subsequently fluxes) are assigned to catalog galaxies from slice sampling the probability histogram.

we assign the catalog galaxy an [O II] luminosity based on the distribution of SDSS galaxies extracted. For catalog galaxies which are placed on the CMD near no, or very few ($1 \leq n < 10$) galaxies we assign it zero [O II] luminosity or the mean luminosity, respectively.

The right panel of Figure 2 shows the CMD of all SDSS galaxies. Two potential catalog galaxies are also placed on the CMD ($M_r, g-r = -17.7,\ 0.49$ and $M_r, g-r = -21.4,\ 1.24$) and indicated by two colored boxes. The histograms show in the Figure's left panel shows the probability density histograms of the Log [O II] luminosity for the SDSS galaxies in the 2D bin. We sample the distribution and assign each catalog galaxy an [O II] luminosity which is then converted into a flux.

2.3. *Mock Observations*

Not sure this does a good enough job talking about the two different observations. Tentatively slated to start in the spring of 2016, HETDEX will perform blind spectroscopy (R $\sim$ 750 in 3500 $-$ 5500 Å) over two fields along the celestial equator. The 300 degree^2, spring field and 120 degree^2, fall field will have no preselected targets. Using VIRUS on the 10-m Hobby-Eberly Telescope (HET; Ramsey et al. 1998) the completed survey is expected to have an overall fill-factor of 1/4.5, meaning that the entire area could be covered with 4.5 dithers of the entire survey.

The spectral coverage allows for the detection of [O II] ($\lambda\lambda$3727 $-$ 3729 Å doublet) emitters to $z \sim 0.5$ and Ca H (λ3968.5 Å) and K (λ3933.7 Å) absorption features to $z \sim 0.4$. HETDEX is expected to detect sources with continuum brighter than 22 mag in g, and emission line strengths above 3.5×10^{-17} erg s^{-1} cm^{-2}. So we "observe" $z < 0.4$ galaxies which meet either the emission line or the magnitude limit. Galaxies $0.4 < z < 0.5$ are only observed if their emission line strength is sufficient.

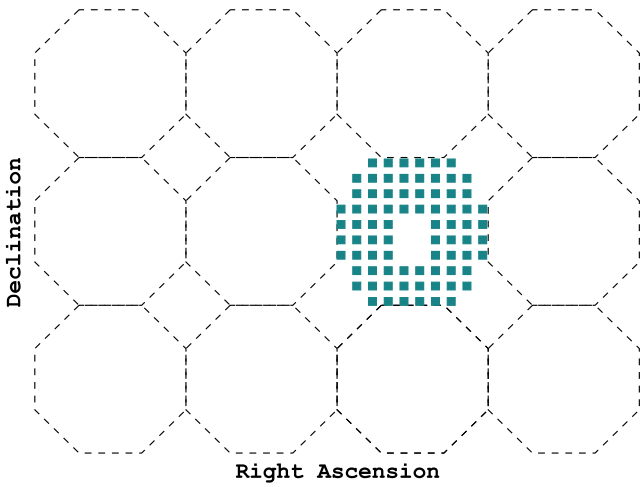

FIG. 3.— Representative observation tiling scheme for the HETDEX 16′ × 16′ pointings. Each colored square is a single VIRUS IFU and the dashed octagons approximate the size of a single observation. See the text for more details.

In this work we consider two separate observation cases. The first are targeted observations where we select each galaxy cluster and "observe" each galaxy within 8′ of the center. The second is a survey case where observations which are blind to the positions of the clusters are conducted. In both cases, our "observations" consist of placing masks down onto the Buzzard "truth" catalogs and selecting all, $z < 0.5$ also meeting sensitivity limits, galaxies which lie underneath. Each mask is created to accurately reproduce the HETDEX IFU pattern, see

Figure 3. The pattern consists of 78 IFUs, which are comprised of 448 optical fibers subtending a $50'' \times 50''$ region on the sky (Kelz et al. 2014). The inter-IFU spacing is also $50''$ spanning a total area of $16' \times 16'$ on the sky.

The individual IFUs have a fill-factor of 1/3, which will be completely filled with three dithers of the telescope at each pointing. This means that when selecting galaxies from the Buzzard catalog we assume an observation for all galaxies laying within a colored, IFU square in Figure 3. This should be updated with the fiber collisions. Galaxies which lie between the IFUs are missed, as well as the galaxies which lie between the pointings, as there is no overlap between one pointing and the next. To cover the 375.67 degree^2 field of the Buzzard catalog we require 5370 pointings where 0.015 degree^2 of each pointing is covered by an IFU. The total area of the sky covered by an IFU is 80.80 degree^2 which gives a filling factor of 1/4.65 slight decreased from the expected filling factor of 1/4.5.

3. RECOVERY OF PARAMETERS

In the following sections, we outline the methods we use to derive the dynamical properties of the galaxy clusters in our sample. This is not meant to be an exhaustive study of the different methods used to recover these parameters. The following is, in many cases, a subset of the available methods to derive any single parameter. The specific choice of method may improve or diminish the accuracy of the recovered parameter, but the methods chosen were to facilitate comparison with observational studies.

3.1. *Cluster Redshift*

The accurate determination of the cluster redshift (z_c) is crucial to the reliability of all following measurements. An incorrect cluster redshift introduces errors into the measured line of sight velocity (LOSV) and corresponding dispersion, which, in turn, contributes to errors associated with dynamical mass and radius.

In simple terms, the cluster redshift is the mean of the redshifts of all galaxies associated with the cluster. However, because the standard mean can be quite sensitive to outliers or otherwise contaminated data, we require a more resistant statistic, and turn to the biweight location estimator (Beers et al. 1990) which provides improved performance.

3.2. *Line of Sight Velocity Dispersion*

We first calculate the line of sight velocity (LOSV) to each galaxy, where

$$LOSV = c\frac{z - z_c}{1 + z_c} \tag{1}$$

and c is the speed of light in km s^{-1}, z is the redshift of the individual galaxy, and z_c is the overall cluster redshift described in the previous section.

The unbiased estimation of a standard deviation (a measure of statistical dispersion) from these LOSVs is a technically involved problem. At first, we require that our estimator be unbiased in that the dispersion estimation is equal to the true dispersion regardless of the number of points sampled, although, in practice this rarely occurs. The most commonly used estimate is the corrected sample standard deviation, given by:

$$s = \sqrt{\frac{1}{n-1}\sum_{i=1}^{n}(x_i - \bar{x})^2} \tag{2}$$

with $\{x_1, x_2, ..., x_n\}$ being the random sample and $\bar{x}$ the sample mean. The corrected sample standard deviation has the advantage in that it is unbiased (as opposed to the population standard deviation which is biased), but the removal of bias relies on knowing *a priori* the underlying distribution from which the sample is drawn. An estimator which correctly estimates a standard deviation for a sample drawn from a wide range of distributions and is not adversely effected by outliers is said to be robust. An estimator which correctly identifies the standard deviation, even when a number of points are replaced by different values is said to be resistant.

In our situation, a resistant estimator becomes critical as it minimizes the effect of outliers which the inclusion of non-cluster members have on the measured dispersion. Beers et al. (1990) present both a robust and resistant estimation of scale (yet another term for statistical dispersion) called the biweight scale estimator, which has been widely accepted by the community (e.g., Milvang-Jensen et al. 2008; Owers et al. 2011; Murphy et al. 2011 and many others). It is given by

$$\sigma_{BI} = \sqrt{N_{members}\frac{\sum_{|u_i|<1}(1-u_i^2)^4(v_i - \bar{v})^2}{D}} \tag{3}$$

with v_i, the proper velocities, $\bar{v}$, the average of the proper velocities,

$$D = \sum_{|u_i|<1}(1-u_i^2)(1-5u_i^2) \tag{4}$$

with u_i being the biweight weighting and defined as:

$$u_i = \frac{v_i - \bar{v}}{9\mathrm{MAD}(v_i)} \tag{5}$$

where MAD is the median absolute deviation. Ruel et al. (2014) note, however, that the biweight scale estimator is biased and suggest a correction of $1/(D-1)$ to σ_{BI} referring to it as the biweight sample variance. We adopt this method for clusters with at least 15 members. For clusters with fewer than 15 members, we adopt the gapper scale estimator (Beers et al. 1990) which is shown to accurately recover the dispersion for as few as 5 member galaxies (Hou et al. 2009).

There are several situations which can adversely effect the quality of our velocity dispersion measurement. The first is due to the nature of our observations. Because the HETDEX survey has a 1/4.5 fill factor (see Section 2.3), there will be many situations where we will not have full spectroscopic information for a cluster. Some clusters could also have intrinsic velocity distributions where the observations of only a few members could result in a LOSVD which differs by large percent. This gives rise to clusters along a fixed mass having a large range of possible LOSVDs. Saro et al. (2013) find this effect to be most pronounced for clusters with fewer than 30 members, and

Ruel et al. (2014) show the effect is a net increase in scatter of about 5% compared to clusters with greater than 30 members. This section was adapted, pretty heavily from Ruel2014. Is that cool?

A second effect, unique to works such as this, is the difference between the LOSVD computed between dark matter halos and the galaxies that occupy them, the so-called velocity bias (e.g., Evrard et al. 2008; White et al. 2010). This effect is assumed to be small ($\sim 5\%$) and for this work we assume there is no bias, or that the galaxies perfectly trace the velocity distribution.

3.3. *Dynamical Mass*

Recently, the relationship between the LOSVD and dynamical mass has been the focus of several studies (e.g., Evrard et al. 2008; Saro et al. 2013; Sifón et al. 2013; van der Burg et al. 2014), and a best fitting relationship for the mass enclosed by r_{200c} of the form

$$M_{200c} = \frac{10^{15}}{h(z)} \left(\frac{\sigma_{1D}}{A_{1D}} \right)^{1/\alpha} \mathrm{M}_{\odot} \tag{6}$$

with A_{1D} = 1040-1140 km s^{-1} (Munari et al. 2013; referred to as σ_{15} in Evrard et al. 2008 and other works), $\alpha = 1/3$, $h(z) = H(z)/100$, and σ_{1D} is the LOSVD of the velocity tracers (dark matter particles, subhalos or galaxies).

The choice A_{1D} and α varies between studies (e.g., Munari et al. 2013; van der Burg et al. 2014) and should be calibrated on a individual basis. To do this, we randomly select 47494, $z < 0.5$ clusters composed of 36000 10^{13}, 6000 10^{14} and two 10^{15} M$_{\odot}$ halos. We perform a linear fit to the $\sigma_{1D} - M_{200}$ values allowing both A_{1D} and α to vary. We find best fitting parameters of $A_{1D} = 1117.9$ km s^{-1} and $\alpha = 0.3297$, both of which are very near the values from Evrard et al. (2008) of $A_{1D} = 1082.9 \pm 4.0$ km s^{-1} and $\alpha = 0.3361$. Therefore, we chose to adopt the parameters from Evrard et al. (2008) to better facilitate with other simulations (e.g., Old et al. 2014), and observational studies (e.g., Brodwin et al. 2010).

4. RESULTS

4.1. *Recovery of Clusters*

The results of this work come in two broad sections. The accuracy of which we determine each cluster's LOSVD and dynamical mass, and the probability given a determined mass it is the correct mass. We test two different observation strategies with ideal and realistic information about the membership of the observed galaxies. Ideal information is knowing the exact membership of the galaxies, and realistic information relies on methods to determine the membership. The results of this section a shown in Figures XXX and Figures XXX for the LOSVD and masses respectively.

4.2. *Targeted, Ideal Observations*

4.3. *Targeted, Realistic Observations*

4.4. *Blind, Ideal Observations*

4.5. *Blind, Realistic Observations*

We compare the calculated cluster redshifts to the true redshift ($z_{c,true}$) for 114903 galaxies comprising 1379 unique halos, and we find a RMS$[\Delta z/(1 + z_{c,true})] = 4 \times 10^{-4}$ where $\Delta z = z_{c,true} - z_c$. The RMS using just the regular mean is 3.8e-4 which is only slightly better than the biweight. I don't think that will be the case when we get more complicated things.

Lorem ipsum dolor sit amet, consectetur adipisicing elit, sed do eiusmod tempor incididunt ut labore et dolore magna aliqua. Ut enim ad minim veniam, quis nostrud exercitation ullamco laboris nisi ut aliquip ex ea commodo consequat. Duis aute irure dolor in reprehenderit in voluptate velit esse cillum dolore eu fugiat nulla pariatur. Excepteur sint occaecat cupidatat non proident, sunt in culpa qui officia deserunt mollit anim id est laborum.

5. SUMMARY

Lorem ipsum dolor sit amet, consectetur adipisicing elit, sed do eiusmod tempor incididunt ut labore et dolore magna aliqua. Ut enim ad minim veniam, quis nostrud exercitation ullamco laboris nisi ut aliquip ex ea commodo consequat. Duis aute irure dolor in reprehenderit in voluptate velit esse cillum dolore eu fugiat nulla pariatur. Excepteur sint occaecat cupidatat non proident, sunt in culpa qui officia deserunt mollit anim id est laborum.

The authors also wish to thank the anonymous referee whose comments and suggestions significantly improved both the quality and clarity of this work. We also thank Steven W. Crawford for many helpful discussions. This research made use of This research made use of APLpy, an open-source plotting package for Python hosted at http://aplpy.github.com; the IPython package (Perez & Granger 2007); matplotlib, a Python library for publication quality graphics (Hunter 2007). Funding for the SDSS and SDSS-II has been provided by the Alfred P. Sloan Foundation, the Participating Institutions, the National Science Foundation, the U.S. Department of Energy, the National Aeronautics and Space Administration, the Japanese Monbukagakusho, the Max Planck Society, and the Higher Education Funding Council for England. The SDSS Web Site is http://www.sdss.org/. The SDSS is managed by the Astrophysical Research Consortium for the Participating Institutions.

REFERENCES

Abell, G. O. 1958, ApJS, 3, 211
Acquaviva, V., Gawiser, E., Leung, A. S., & Martin, M. R. 2014, Proc. Int. Astron. Union, 10, 365
Alam, S., Albareti, F. D., Prieto, C. A., et al. 2015, ApJS, 219, 12
Annis, J., Soares-Santos, M., Strauss, M. A., et al. 2014, ApJ, 794, 120
Beers, T. C., Flynn, K., & Gebhardt, K. 1990, AJ, 100, 32
Behroozi, P. S., Wechsler, R. H., & Wu, H.-Y. 2013, ApJ, 762, 109
Blanton, M. R., Dalcanton, J., Eisenstein, D., et al. 2001, AJ, 121, 2358
Bocquet, S., Saro, A., Mohr, J. J., et al. 2015, ApJ, 799, 214
Brodwin, M., Ruel, J., Ade, P. A. R., et al. 2010, ApJ, 721, 90
Carlstrom, J. E., Ade, P. A. R., Aird, K. A., et al. 2011, Publ. Astron. Soc. Pacific, 123, 568

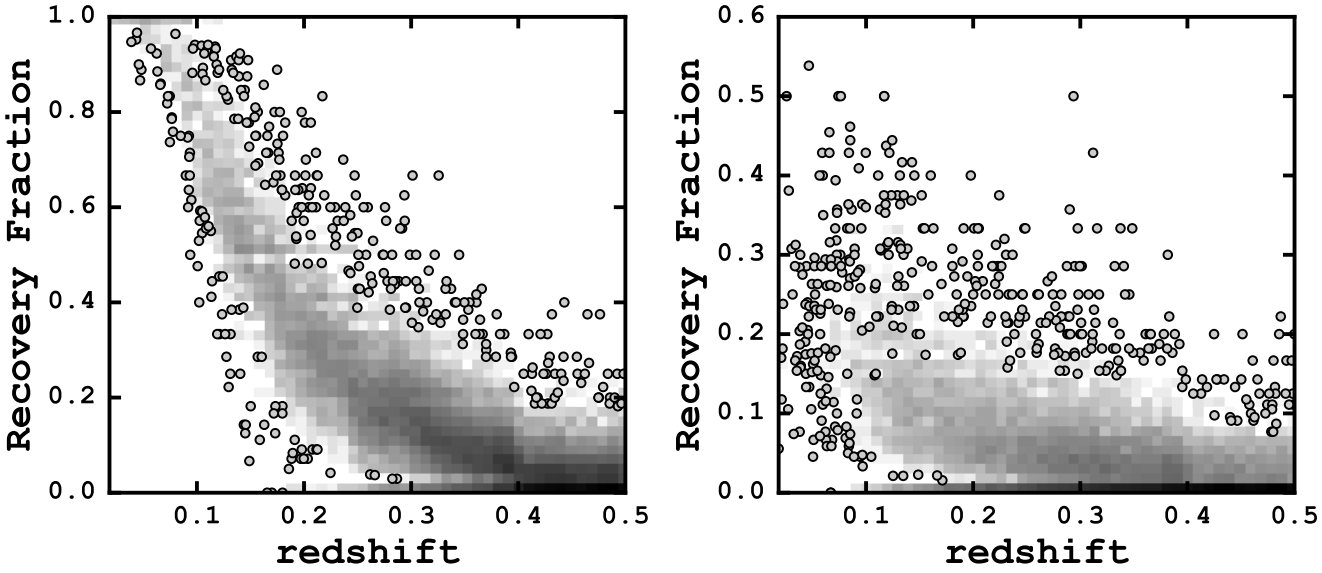

FIG. 4.— *Left*: CMD of 503113 $z < 0.2$ galaxies take from the SDSS DR12 where the shading scales with the density of points. The two boxes show regions containing potential catalog galaxies. *Right*: Probability histograms of the Log [O II] luminosity for the SDSS galaxies located in the two highlighted regions on the right. New [O II] luminosity (and subsequently fluxes) are assigned to catalog galaxies from slice sampling the probability histogram.

Chabrier, G. 2003, Publ. Astron. Soc. Pacific, 115, 763
Crocce, M., Pueblas, S., & Scoccimarro, R. 2006, MNRAS., 373, 369
Eisenstein, D. J., Zehavi, I., Hogg, D. W., et al. 2005, ApJ, 633, 560
Evrard, A. E., Bialek, J., Busha, M., et al. 2008, ApJ, 672, 122
Hill, G. J., Gebhardt, K., Komatsu, E., et al. 2008, Panor. Views Galaxy Form. Evol. ASP Conf. Ser., 399
Hill, G. J., Tuttle, S. E., Lee, H., et al. 2012, in Ground-based Airborne Instrum. Astron. IV. Proc. SPIE, ed. I. S. McLean, S. K. Ramsay, & H. Takami, Vol. 8446, 84460N
Hou, A., Parker, L. C., Harris, W. E., & Wilman, D. J. 2009, ApJ, 702, 1199
Hunter, J. D. 2007, Comput. Sci. Eng., 9, 90
Kelz, A., Jahn, T., Haynes, D., et al. 2014, in Proc. SPIE, ed. S. K. Ramsay, I. S. McLean, & H. Takami, Vol. 9147, 914775
LSST Dark Energy Science Collaboration. 2012, arXiv Prepr. arXiv1211.0310, 133
Mantz, A., Allen, S. W., Rapetti, D., & Ebeling, H. 2010, MNRAS., 406, no
Mantz, A. B., Allen, S. W., Morris, R. G., et al. 2015, MNRAS., 449, 199
Milvang-Jensen, B., Noll, S., Halliday, C., et al. 2008, Astron. Astrophys., 482, 419
Munari, E., Biviano, A., Borgani, S., Murante, G., & Fabjan, D. 2013, MNRAS., 430, 2638
Murphy, J. D., Gebhardt, K., & Adams, J. J. 2011, ApJ, 729, 129
Murray, S., Power, C., & Robotham, A. 2013, Astron. Comput., 3-4, 23
Neal, R. M. 1997, Markov Chain Monte Carlo Methods Based on 'Slicing' the Density Function, Tech. rep., Department of Statistics, University of Toronto, Toronto, doi:10.1.1.48.886
Oke, J. B. 1974, ApJS, 27, 21
Old, L., Skibba, R. A., Pearce, F. R., et al. 2014, MNRAS., 441, 1513
Owers, M. S., Randall, S. W., Nulsen, P. E. J., et al. 2011, ApJ, 728, 27
Perez, F., & Granger, B. E. 2007, Comput. Sci. Eng., 9, 21
Planck Collaboration. 2013, Astron. Astrophys., 571, 19
Ramsey, L. W., Adams, M. T., Barnes III, T. G., et al. 1998, in Proc. SPIE, Vol. 3352, 34–42
Reddick, R. M., Wechsler, R. H., Tinker, J. L., & Behroozi, P. S. 2013, ApJ, 771, 30
Robotham, A. S. G., Norberg, P., Driver, S. P., et al. 2011, MNRAS., 416, 2640
Rozo, E., Rykoff, E. S., Bartlett, J. G., & Melin, J.-B. 2015, MNRAS., 450, 592
Rozo, E., Wechsler, R. H., Rykoff, E. S., et al. 2010, ApJ, 708, 645
Ruel, J., Bazin, G., Bayliss, M., et al. 2014, ApJ, 792, 45
Rykoff, E. S., Koester, B. P., Rozo, E., et al. 2012, ApJ, 746, 178
Rykoff, E. S., Rozo, E., Busha, M. T., et al. 2014, ApJ, 785, 104
Saro, A., Mohr, J. J., Bazin, G., & Dolag, K. 2013, ApJ, 772, 47
Sehgal, N., Trac, H., Acquaviva, V., et al. 2011, ApJ, 732, 44
Sifón, C., Hoekstra, H., Cacciato, M., et al. 2015, Astron. Astrophys., 575, A48
Sifón, C., Menanteau, F., Hasselfield, M., et al. 2013, ApJ, 772, 25
Springel, V. 2005, MNRAS., 364, 1105
Sunyaev, R. A., & Zeldovich, Y. B. 1972, Comments Astrophys. Sp. Phys., 4
Swetz, D. S., Ade, P. A. R., Amiri, M., et al. 2011, ApJS, 194, 41
The Dark Energy Survey Collaboration. 2005, eprint arXiv:astro-ph/0510346, 42
Tinker, J., Kravtsov, A. V., Klypin, A., et al. 2008, ApJ, 688, 709
van der Burg, R. F. J., Muzzin, A., Hoekstra, H., et al. 2014, Astron. Astrophys., 561, A79
Vanderlinde, K., Crawford, T. M., de Haan, T., et al. 2010, ApJ, 722, 1180
White, M., Cohn, J. D., & Smit, R. 2010, MNRAS., 408, 1818